JOURNAL OF GEOPHYSICAL RESEARCH, VOL. 102, NO. D22, PAGES 25,737–25,749, NOVEMBER 27, 1997

Evaluation of model-simulated upper troposphere humidity using 6.7 μm satellite observations

Douglas A. Spangenberg,[1] Gerald G. Mace,[2] Thomas P. Ackerman,
and Nelson L. Seaman
Department of Meteorology, Pennsylvania State University, University Park

Brian J. Soden
Geophysical Fluid Dynamics Laboratory, NOAA, Princeton, New Jersey

Abstract. Use of mesoscale models to simulate details of upper tropospheric relative humidity (UTRH) fields represents an important step toward understanding the evolution of small-scale water vapor structures that are responsible for cirrus growth and dissipation. Because mesoscale model UTRH simulations require initialization and verification and since radiosonde measurements of relative humidity are unreliable in the upper troposphere, we use GOES 6.7 μm water vapor observations to validate the Pennsylvania State University/National Center for Atmospheric Research nonhydrostatic mesoscale model (MM5) simulations of UTRH. To accomplish this task, MM5 temperature and moisture profiles are used in a forward calculation of the clear-sky 6.7 μm brightness temperature ($T_{6.7}$), which is converted into UTRH. A statistical analysis is done to evaluate MM5 simulations of $T_{6.7}$ and UTRH against the GOES 7 observations. For the simulations, an average correlation coefficient of 0.80 was found with a dry bias of 1.6 K. In terms of UTRH, the average correlation coefficient was 0.65 with a dry bias of 3.3%. We also found that MM5 fails to simulate accurately extrema in the UTRH field.

1. Introduction

Gaining a fuller quantitative understanding of the mechanisms that control the water budget in the upper troposphere is an important scientific objective that must be met before improved cloud parameterizations can be developed and implemented in general circulation models [First *International Satellite Cloud Climatology Project* Regional Experiment Project Office, 1994]. Not only do radiatively active cirrus clouds form and dissipate within this environment, but clear-sky longwave cooling to space is significantly modulated by the quantity and location of water vapor in the upper troposphere [*Ackerman et al.*, 1992]. As pointed out by *Westphal et al.* [1996] and others, even though water is one of the most abundant constituents of the atmosphere, it has remained very difficult to measure accurately in the cold temperatures and low vapor pressures of the upper troposphere. Given the strong advective speeds, the tight horizontal gradients, and the nonlinear interactions between scales of motion, even if the water vapor could be measured accurately in the upper troposphere, it would prove difficult to close the water budget with data alone.

Mesoscale atmospheric models designed for numerical weather prediction that use nonhydrostatic codes, nested grids, and four-dimensional data assimilation have proven useful for diagnostic studies of the coupling between atmospheric dynamics and physical processes [*Westphal et al.*, 1996]. However, only a few studies have attempted a quantitative validation of the model's skill and fewer still have attempted to simulate the upper tropospheric water cycle in detail. In this work we attempt to validate upper tropospheric water vapor simulations generated by the Pennsylvania State University/National Center for Atmospheric Research mesoscale model (MM5) [*Dudhia*, 1993] using radiance observations of the 6.7 μm water vapor rotational band observed by the GOES 7 satellite. Previous studies have demonstrated the sensitivity of the 6.7 μm water vapor band to mean upper tropospheric relative humidity (UTRH) [*Schmetz and Turpeinen*, 1988; *Van De Berg et al.*, 1991; *Wu et al.*, 1993]. *Soden and Bretherton* [1993], hereafter referred to as SB93, used 6.7 μm UTRH observations from the geostationary satellite for comparison with general circulation model UTRH simulations to assess model performance.

For this initial study, we adopt the technique of SB93 and consider a 10 day period during the project FIRE II field deployment during November and December 1991. Our goal is not to evaluate the model's microphysical parameterizations; we defer that work to a future paper. However, we do attempt to demonstrate the utility of a detailed forward comparison of mesoscale model output with satellite radiance data and critically examine both the initialization procedure and predictive skill of this mesoscale model for simulating the hydrologic cycle in the upper troposphere.

[1]Now at NASA Langley Research Center, Hampton, Virginia.
[2]Now at Department of Meteorology, University of Utah, Salt Lake City.

Copyright 1997 by the American Geophysical Union.

Paper number 97JD01552.
0148-0227/97/97JD-01552$09.00

2. Analysis Technique

2.1 Mesoscale Model

MM5 is a nonhydrostatic, three-dimensional, limited area, primitive equation model cast in terrain-following sigma coordinates. This model represents the prognostic mass-field variables (pressure, temperature, and mixing ratio) as the sum of a constant base state and perturbation from that base state [*Grell et al.*, 1994]. The model domain used in this study encompasses much of the United States (Figure 1) and has 110x120 grid points, 20 sigma levels, and a 36 km grid spacing. The pressure at the center of the highest sigma layer is typically between 110 and 150 mbar, the center of the lowest sigma layer is approximately 35 m above the surface. Initial conditions and lateral boundary conditions for MM5 consist of three-dimensional, Cressman-type mesoscale analyses supplied by the National Meteorological Center. Owing to the lack of reliable relative humidity reports from radiosondes in the upper troposphere, the relative humidity is initialized to 10% in MM5 levels above 300 mbar. A more detailed description of the MM5 model is given by *Dudhia* [1993] and *Stauffer and Seaman* [1990].

To provide time continuity and dynamic coupling among the modeled fields, a Newtonian-relaxation data-assimilation technique is used in MM5 for this application [*Stauffer and Seaman*, 1990; *Guo*, 1994] whereby the model solutions are nudged toward gridded analyses based on the observations. Radiosonde data (horizontal wind, temperature, and specific humidity) are assimilated every 12 hours while surface data (horizontal wind and specific humidity) are assimilated at 3 hour intervals. The nudging coefficient for the model specific humidity is 25 times smaller than the coefficient for the other variables. As a result, the analyzed specific humidity has a negligible influence on the simulated water vapor field after initialization.

2.2 Geostationary Satellite Observations

We use clear-sky 6.7 μm satellite observations made by the visible infrared spin scan radiometer (VISSR) atmospheric sounder (VAS) on the GOES 7 satellite as a verification data set. The 6.7 μm radiances are observed every 30 min with a nadir resolution of 16 km. During FIRE II, GOES 7 was centered at 75° W longitude. In-flight calibration of the VAS instrument indicates that the random noise in individual VAS observations is about ±0.75 K with biases up to 1.9 K due to calibration uncertainties [*Menzel et al.*, 1981].

To facilitate the comparison of the satellite data with MM5 simulations during FIRE II, we use a version of the GOES data set that has been averaged to a 0.5° latitude by 0.5° longitude grid. This grid encompasses much of the United States and consists of hourly GOES radiance observations taken from 0000 UTC November 24 to 2300 UTC December 3, 1991. Since even thin cirrus clouds are opaque at 6.7 μm, only clear-sky pixels can be used for the analysis of upper tropospheric water vapor. Therefore, the images were carefully screened for cirrus clouds using the technique described by SB93.

SB93 also presented a method to estimate UTRH from geostationary satellite observations of upwelling radiance. They

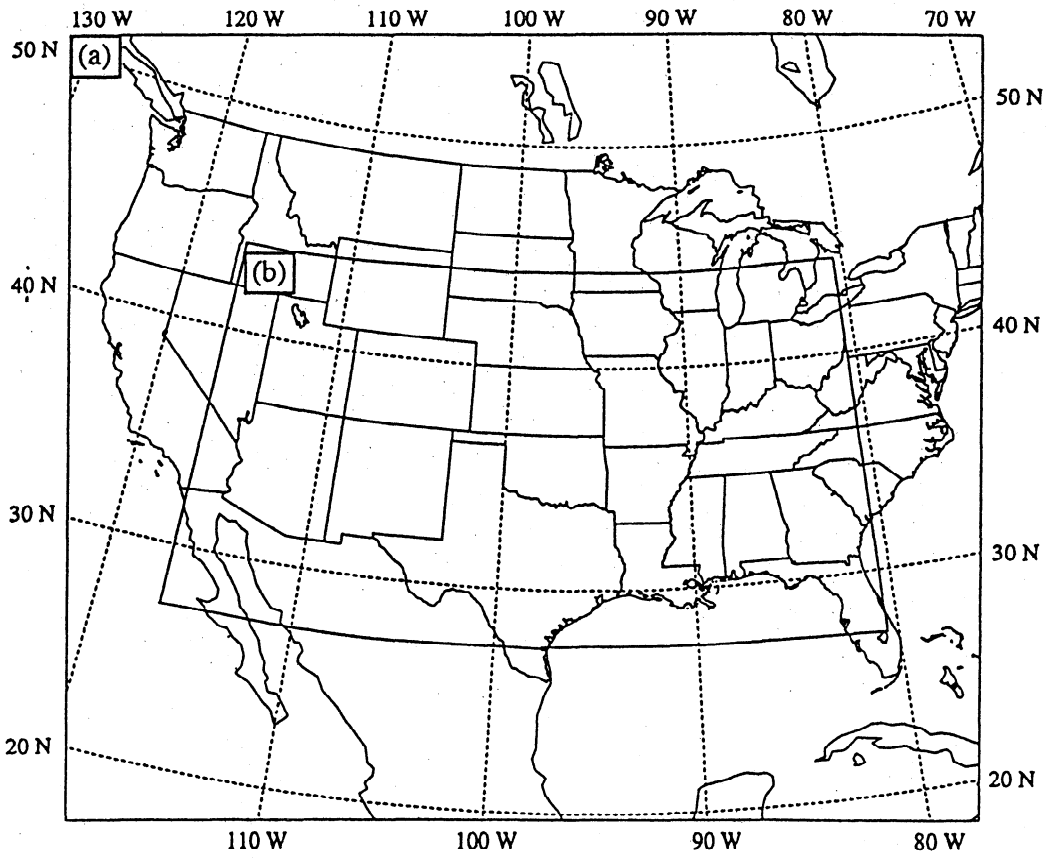

Figure 1. Location of the 36 km mesoscale model (MM5) domain. Outlined area shows the GOES and MM5 latitude by longitude validation grid.

compared values of brightness temperatures in the 6.7 μm band ($T_{6.7}$) from GOES 7 with vertically averaged 200-500 mbar relative humidities from the European Centre for Medium-Range Weather Forecasts (ECMWF) analysis and found that, to within an accuracy of ±1 K or ±8% in UTRH, $T_{6.7} \propto \ln(\mathrm{UTRH}/\cos\theta)$ where θ is the satellite zenith angle. By using July 1987 ECMWF temperature and specific humidity profiles as input to a radiation transfer model, Soden and Bretherton found the regression coefficients relating $T_{6.7}$ to the UTRH. Their equation has the form

$$\ln\left(\frac{UTRH}{\cos\theta}\right) = a + bT_{6.7} \tag{1}$$

where a and b are regression coefficients whose values are 31.50 and 0.115 K^{-1}, respectively. The coefficients for (1) were derived using only July 1987 ECMWF data. Little dependence on seasonal or interannual variations is expected, however, since a large range of temperature and moisture profiles were used in performing the regression. *Soden et al.* [1994] found that during FIRE II the vertical variability in the relative humidity profiles did not appreciably affect the interpretation of UTRH from GOES 6.7 μm observations. Their data suggested that the inferred GOES UTRH is typically within 5% of the relative humidity vertically averaged over the depth of the atmosphere to which the 6.7 μm channel is sensitive.

2.3 GOES-MM5 Comparison Procedure

In order to compare GOES $T_{6.7}$ observations with MM5-simulated output obtained during FIRE II, MM5 temperature and specific humidity profiles are used in a forward calculation of the radiance that would be observed by the satellite sensor. The forward model we use was developed at the University of Wisconsin Cooperative Institute for Meteorological Satellite Studies (CIMMS) and is a 40 pressure level, multivariate regression model based on FASCOD3 line-by-line transmittance calculations [*Soden and Bretherton*, 1993, 1994]. It uses water vapor absorption lines at 6.7 μm, the GOES 7 spectral response function, the satellite zenith angle, and temperature and water vapor profiles to calculate the transmission from each pressure level to the satellite. The derived transmission profile is dependent primarily on water vapor absorption and subsequent emission of thermal radiation in the 6.7 μm wavelength band. Comparison of the CIMSS transmittance model calculations with FASCOD3 line-by-line calculations suggests the CIMSS model is accurate to roughly 1.0-1.5 K. It has been shown in previous studies [*Soden and Bretherton*, 1993; *Wu et al.*, 1993] that the sensitivity of $T_{6.7}$ to variations in UTRH at constant temperature is a factor of 8 larger than the $T_{6.7}$ sensitivity to representative temperature variations at constant UTRH. Therefore, variability in $T_{6.7}$ is taken to represent changes in the mean water vapor concentration in the upper troposphere over the domain being observed.

Using the MM5 temperature and specific humidity profile at each gridpoint, $T_{6.7}$ is computed using the CIMMS model over the entire MM5 domain and the values are interpolated to the 0.5° latitude by 0.5° longitude GOES grid using the bivariate interpolation scheme described by [1978, 1984]. Because a higher degree of small-scale spatial variability is present in the GOES data than in the MM5 model, we found it necessary to smooth the GOES observations. Variability on wavelength scales down to 250 km is common in the GOES data (Figure 3). This variability may represent a combination of noise in the satellite radiometer and small scale water vapor features not resolved by the mesoscale model. The spatial scales present in the MM5 $T_{6.7}$ fields tend to be of the order of 1000 km or greater. As configured here, MM5 does not have sufficient vertical resolution in the upper troposphere (1.5 km) to simulate the laminar mesoscale water vapor features commonly observed. Therefore MM5 relative humidity fields in the upper troposphere develop at the scales of the longwave (5000 km) and shortwave (1000 km) dynamic forcing. We chose a spatial filter [*Mace et al.*, 1994] that removes the spatial variability in the GOES observations below a 1000 km cutoff wavelength. The amplitude response of the filter is depicted in Figure 2. To insure that the GOES data and MM5 output resolve identical spatial scales, both the satellite data and model output are passed through the same filter. Figure 3 shows a comparison of the GOES data before and after smoothing; also shown is the corresponding MM5 output before and after smoothing. The filter removes the small-scale variability in the GOES data while leaving much of the MM5 variability intact.

Four statistics are used to validate the MM5 UTRH simulations. They are represented by the formulae,

$$COR = \frac{N\sum_{i=1}^{N}(o_i s_i) - \left(\sum_{i=1}^{N} o_i \bullet \sum_{i=1}^{N} s_i\right)}{\sqrt{\left[N\sum_{i=1}^{N} o_i^2 - \left(\sum_{i=1}^{N} o_i\right)^2\right] \bullet \left[N\sum_{i=1}^{N} s_i^2 - \left(\sum_{i=1}^{N} s_i\right)^2\right]}} \tag{2}$$

$$bias = \frac{1}{N}\sum_{i=1}^{N}(s_i - o_i) \tag{3}$$

$$BSD = \sqrt{\frac{1}{N}\sum_{i=1}^{N}(s_i - o_i)^2 - \left[\frac{1}{N}\sum_{i=1}^{N}(s_i - o_i)\right]^2} \tag{4}$$

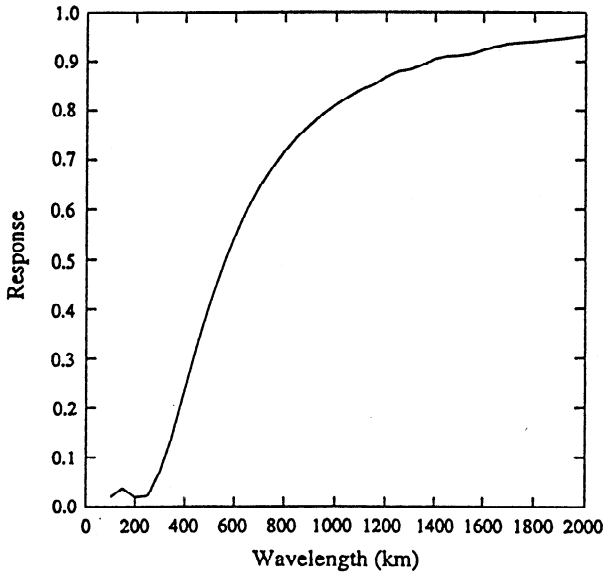

Figure 2. Amplitude response function of the least squares spatial filter discussed in the text.

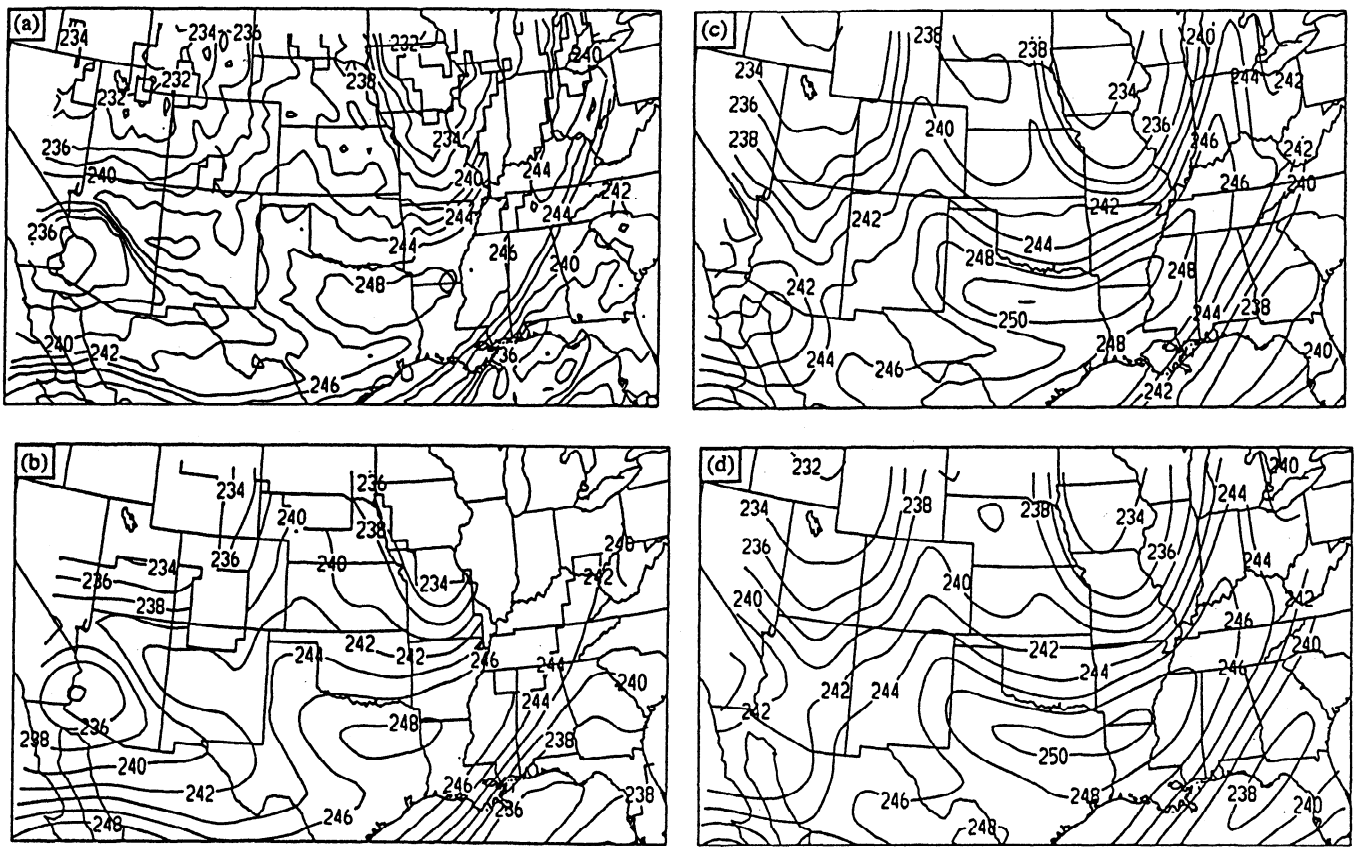

Figure 3. Analyzed GOES and MM5 clear-sky 6.7 m brightness temperatures (degrees Kelvin) for 0000 UTC November 24, 1991. Rectangular-shaped boxes with missing GOES data represent regions contaminated by cirrus clouds. (a) GOES-unsmoothed data,; (b) GOES-smoothed data,; (c) MM5-unsmoothed data,; and (d) MM5-smoothed data.

$$slope = \frac{N\sum_{i=1}^{N}(o_i s_i) - \left(\sum_{i=1}^{N} o_i \bullet \sum_{i=1}^{N} s_i\right)}{N\sum_{i=1}^{N} o_i^2 - \left(\sum_{i=1}^{N} o_i\right)^2} \quad (5)$$

where COR is the linear correlation coefficient, bias is the mean difference between the GOES- and MM5-simulated values, BSD is the standard deviation of bias, and slope is the slope of the linear regression line fitted through a scatterplot of the MM5 and GOES observations. The number of grid points used in the statistical evaluation at any time is represented by N; s and o are the MM5-simulated and GOES-observed $T_{6.7}$ and UTRH values, respectively. We also examine the correlation coefficient for the horizontal shift in the MM5 grid relative to the GOES grid that produces the best correlation between the model output and satellite data [*Anthes*, 1983; *Tarbell et al.*, 1981]. The comparison of the shifted grid allows us to evaluate if the model predicted the correct water vapor pattern shifted spatially from the pattern that actually occurred.

With the GOES observations and MM5 output interpolated onto a common grid and filtered to identical spatial scales, we carry out an evaluation of the model simulations for the period from 0000 UTC November 24, 1991 to 2300 UTC December 3, 1991. During that 10 day period, output from eight overlapping MM5 runs is used. The output from each model run consists of hours 12 to 47 of overlapping simulations (hours 1-11 are used for model spinup after initialization). Equation (1) is used to compute the UTRH in terms of $T_{6.7}$ for both the model output and satellite data. The statistical evaluation of MM5 is then performed by comparing hourly GOES $T_{6.7}$ and UTRH data with MM5 $T_{6.7}$ and UTRH output at each grid point over the computational domain. Figure 1 shows the geographical location of the latitude-longitude domain used for the MM5-GOES comparison.

3. Results

The synoptic pattern over the central United States was quite varied during this period and represented a rather typical autumn transition period. During November 24, a high-amplitude flow pattern existed with ridges in the western Atlantic and in the eastern Pacific. The main trough axis was present over the Mississippi and Tennessee River valleys. Broad northwesterly flow existed over most of the analysis domain and was generally dry in the upper troposphere because of large-scale subsidence. By November 25, 1991, the high amplitude pattern began to deamplify as weak disturbances moved through the central United States. Strong gradients of UTRH were present in the

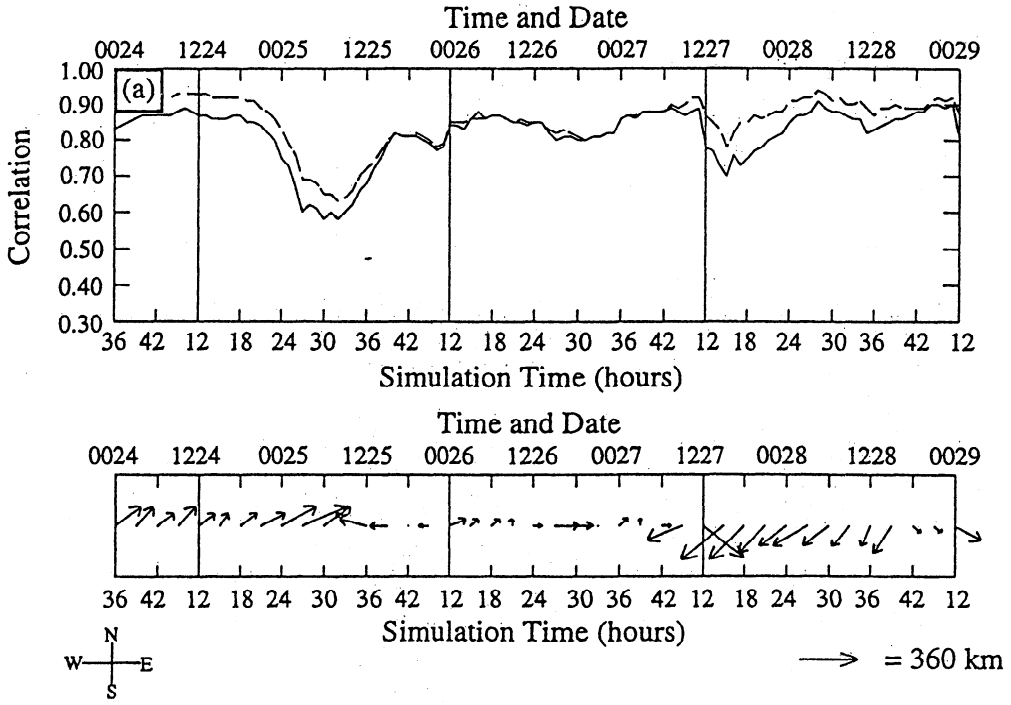

Figure 4. Time sequence of the MM5 versus GOES correlation coefficient from November 24 to December 3, 1991 (solid line), along with the correlation coefficient for that spatial shift in the MM5 grid that produces the best agreement with the GOES data (dashed line). Also shown is the time series of MM5 shift vectors, indicating the magnitude and direction the MM5 grid was shifted to produce the best correlations with the GOES data. Vertical lines indicate the beginning of a new model run. The model valid time and date are shown on top of each graph using a four-digit convention (For example, 0024 is 0000 UTC November 24). (a) 0000 UTC November 24 to 0000 UTC November 29, 1991; (b) 0000 UTC November 29 to 2300 UTC December 3, 1991; (c) UTRH 0000 UTC November 24 to 0000 UTC November 29, 1991; and (d) UTRH 0000 UTC November 29 to 2300 UTC December 3, 1991.

southern portion of the analysis domain while the northern sections moistened substantially because of the progressive disturbances that were propagating eastward in an increasingly zonal flow. The period of November 26 and 27 was a transition from a nearly zonal jet to a strong southwesterly jet as a high-amplitude trough deepened in western North America, and by November 28, UTRH had increased substantially over most of the domain. Only the inter mountain West was relatively dry. During the next week, jet maxima and large weather systems propagated through this pattern and resulted in strong, progressive gradients and small-scale variability in the UTRH. Dry northwesterly flow returned to the region by December 3.

3.1 Linear Correlation Coefficient

A time series of the correlation coefficient for the MM5-simulated $T_{6.7}$ and UTRH output is shown in Figure 4; this statistic is computed using (2). The shift vectors show the magnitude and direction that the MM5 grid was shifted to produce the best correlations. Overall, the correlation coefficients tend to range from 0.8 to 0.9 for $T_{6.7}$ and from 0.65 to 0.75 for UTRH. The model correlates strongly with the satellite observations during November 24. During this time, the dynamic forcing was weak, and the spatial variability in UTRH was small. By November 25, when the upper flow became more progressive and moisture increased in the northern portions of the analysis domain, COR decreased substantially. MM5 did not simulate well the increasing moisture in the north and the strong spatial gradients in the south. After the COR minimum at 0600 UTC November 25, this statistic increased slowly until November 28 reaching a maximum early on the 28th. A slow but steady decrease is noted thereafter. The low correlation calculated for December 2 is due to most of the domain being cloud covered. With respect to each individual model run, the correlation coefficient shows no clear trend from beginning to end of a forecast cycle. The onset of the strong southwesterly jet is evident by the increase in the shift vectors after 1200 UTC November 27. However, shifting the model grid results in a substantial increase in COR only on November 28 and December 2.

3.2 Model Bias

The bias (equation (3)) is defined to be the average of the difference between simulated and observed values of $T_{6.7}$ and UTRH. For a perfect model solution, the bias is zero. Figure 5 depicts a time series of the bias found in MM5-UTRH simulations. Also shown is the value of the bias obtained by shifting the MM5 grid relative to the GOES grid according to the shift vectors in Figure 4. The MM5 bias is predominantly negative, indicating that the model is biased toward lower upper tropospheric relative humidities, with biases mostly between -1 and -8%. This dry bias is typically between 0.5 and 3.0 K in terms of $T_{6.7}$. During the first half of the simulation period, the bias tends to be very sensitive to the model initialization. This is especially evident with the model output beginning at 1200

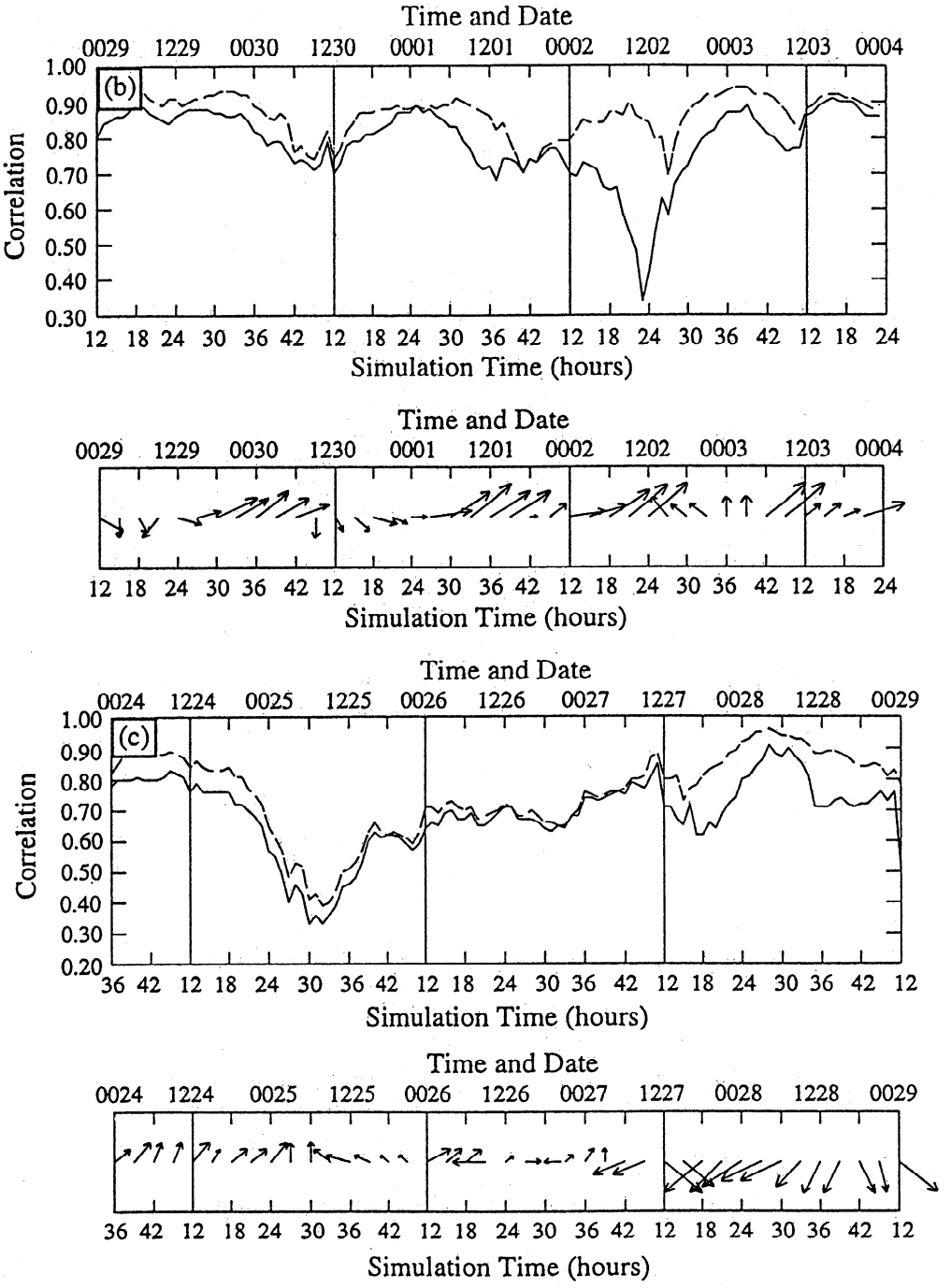

Figure 4. (continued) Time sequence of the MM5 versus GOES correlation coefficient from November 24 to December 3, 1991 (solid line), along with the correlation coefficient for that spatial shift in the MM5 grid that produces the best agreement with the GOES data (dashed line). Also shown is the time series of MM5 shift vectors, indicating the magnitude and direction the MM5 grid was shifted to produce the best correlations with the GOES data. Vertical lines indicate the beginning of a new model run. The model valid time and date are shown on top of each graph using a four-digit convention (For example, 0024 is 0000 UTC November 24). (a) 0000 UTC November 24 to 0000 UTC November 29, 1991; (b) 0000 UTC November 29 to 2300 UTC December 3, 1991; (c) UTRH 0000 UTC November 24 to 0000 UTC November 29, 1991; and (d) UTRH 0000 UTC November 29 to 2300 UTC December 3, 1991.

UTC November 24 (initialized at 0000 UTC November 24). Recall that during this time, COR reached a minimum at 06 UTC and increased thereafter. The dry bias in the model also decreases and approaches zero by 0000 UTC November 26. The bias then increases dramatically as the output from the run initialized at 1200 UTC November 25 is used and does not recover until the latter half of November 28. The model bias remains between 0 and -4% during the remainder of the simulation period.

Only on the 28th, does shifting the model grid to produce the

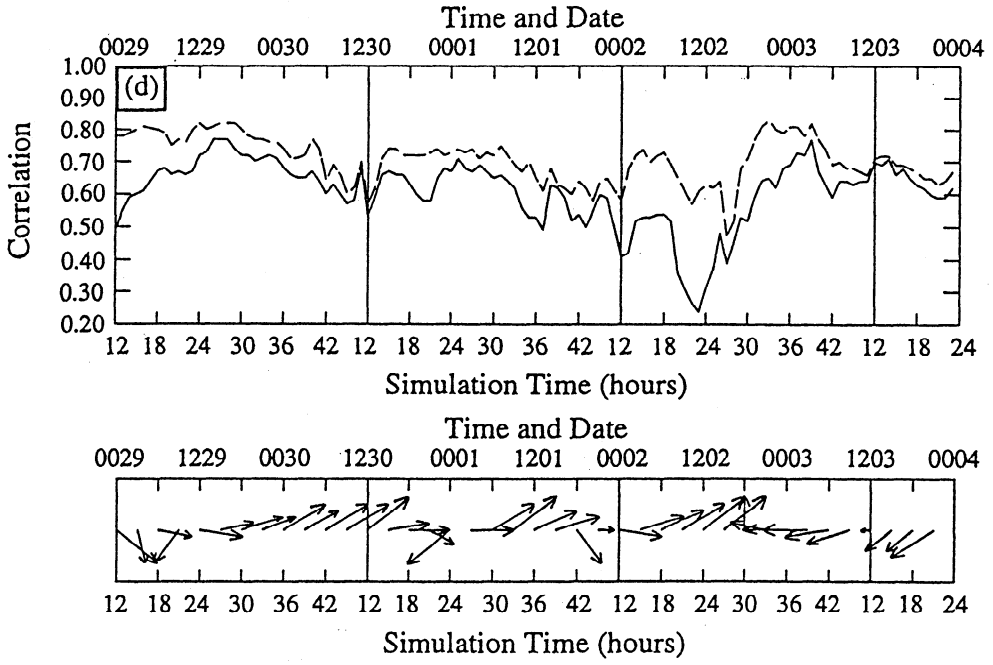

Figure 4. (continued)

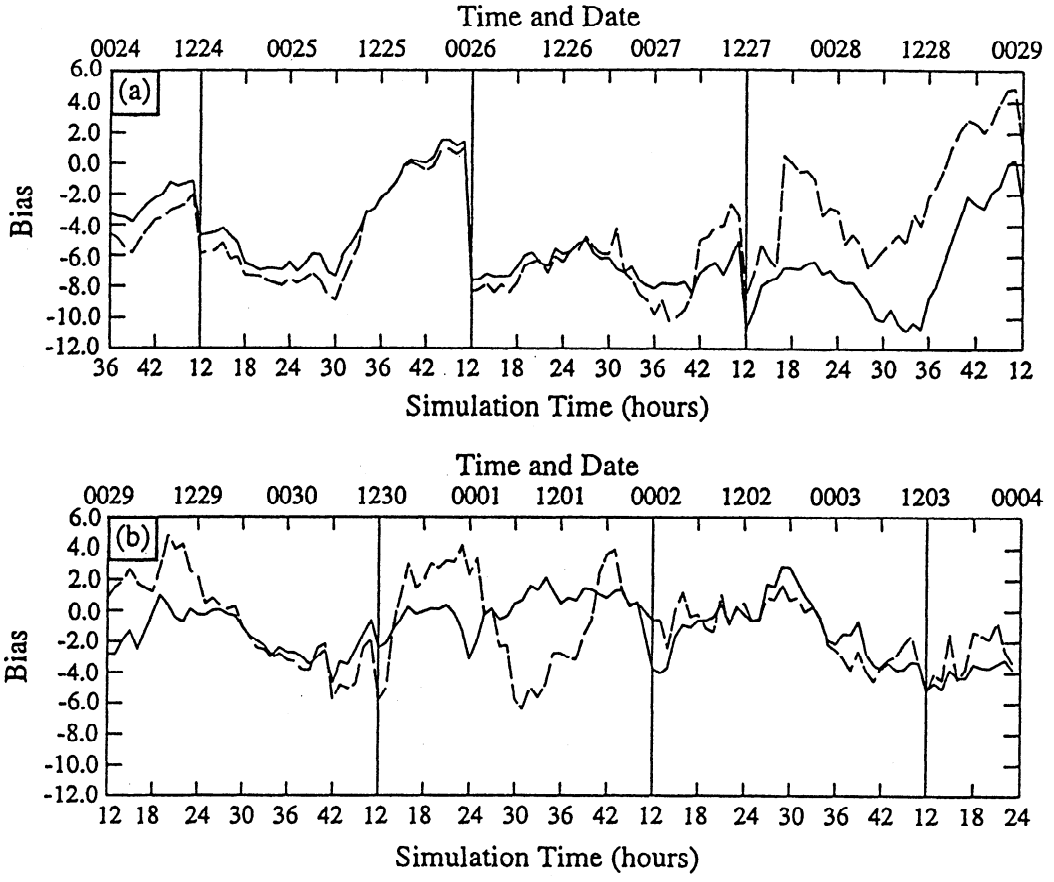

Figure 5. Time series of the MM5 and upper tropospheric relative humidity (UTRH) bias from November 24 to December 3, 1991 (solid line) along with the bias corresponding to a shift in the MM5 grid as denoted by the shift vectors in Figure 4 (dashed line). Vertical lines indicate the beginning of a new model run. The model valid time and date is shown on top of each graph using a four-digit convention (for example, 0024 is 0000 UTC November 24). (a) 0000 UTC November 24 to 0000 UTC November 29, 1991; (b) 0000 UTC November 29 to 2300 UTC December 3, 1991

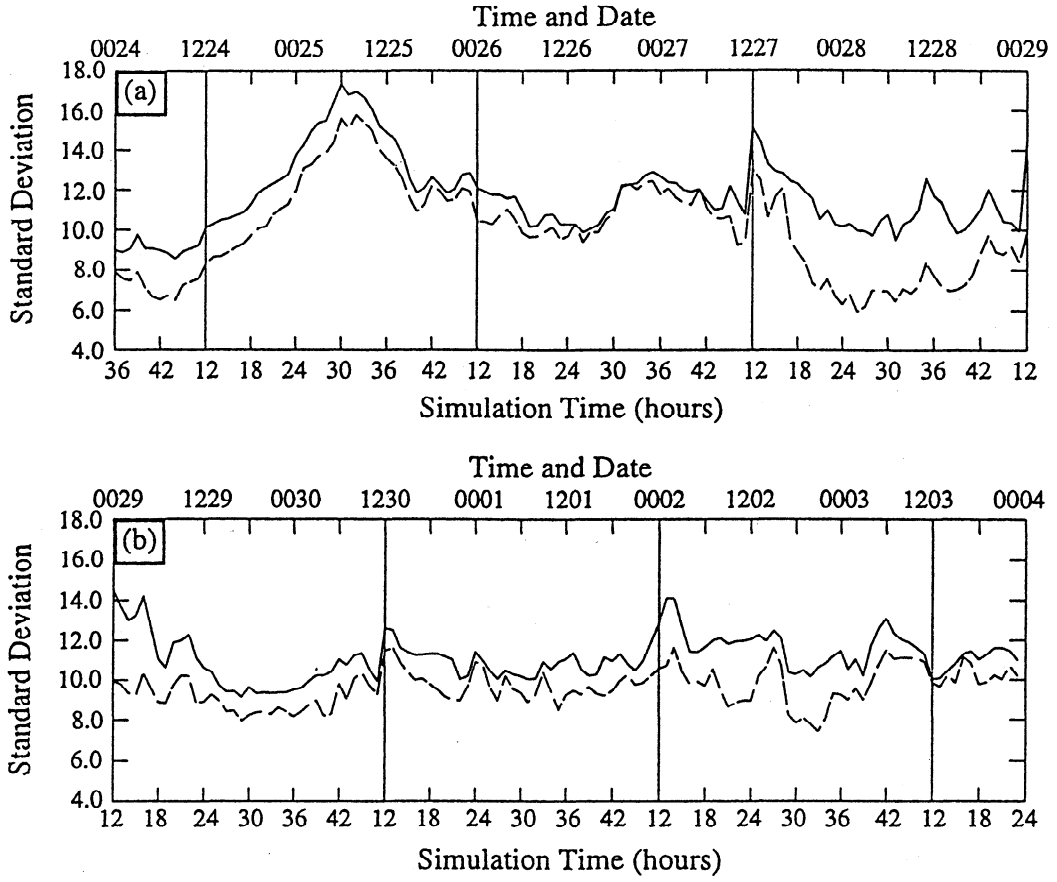

Figure 6. Same as Figure 5 but for the MM5 UTRH bias standard deviation. (a) 0000 UTC November 24 to 0000 UTC November 29, 1991; (b) 0000 UTC November 29 to 2300 UTC December 3, 1991.

highest correlation coefficient substantially reduce the bias. During this period, a uniform northeast-southwest upper tropospheric water vapor gradient was present over the southern United States, with higher water vapor values to the northeast. Although MM5 simulates the gradient, the model UTRH field is displaced too far northeast (not shown). With a southwest shift of the MM5 grid, the correlation coefficient improves, and the bias is removed.

The persistent dry bias in the MM5 upper troposphere is almost certainly due to the model being initialized with 10% relative humidity above 300 mbar. During the latter half of the simulation period, the model dynamics were able to realistically moisten the upper troposphere by the 12th hour of integration when we begin comparison with GOES data. During the first half of the simulation period, however, the dynamic forcing was relatively weak, and the model took nearly the full 48 hours to recover from the unrealistic initialization. This is particularly evident on the 25th and 28th. On November 26, the large model bias remains nearly constant since MM5 simulated poorly an amplifying trough and low pressure area developing in the midwestern United States [*Mace*, 1994].

3.3 Bias Standard Deviation

The standard deviation of the bias (equation (4)) is a measure of the amount of scatter between the GOES observations and the MM5 output. For a perfect model simulation, BSD=0. Figure 6 depicts the time series of the UTRH BSD along with BSD for the shift in the model grid having maximum correlation. The BSD averages to approximately 12% over the 10 day period (roughly 3 K in terms of $T_{6.7}$). Maxima in BSD tend to occur at the beginning of a particular model run and improve only slightly during the simulation. This is particularly notable at 12 UTC November 27 and at 0000 UTC November 29. In both cases BSD begins near 14% and drops to around 10% by the 24th hour of the simulation. The bias standard deviation always improves for the appropriate shift in the MM5 grid that produces maximum correlation, although only on November 28 does this lead to a notable reduction in the scatter between observation and simulation. In general, no discernible trends in the bias standard deviation exist from beginning to end of each forecast period, indicating that any spatial or timing errors in the model do not grow as the forecast is run out to 47 hours. A larger scatter in the MM5 versus GOES data is seen from 0000-1500 UTC November 25, corresponding to the same time when correlation coefficients are lowest.

3.4 Slope of the Linear Regression Line

The final statistic used to evaluate MM5 predictions of UTRH is the slope of the line obtained from a linear regression between the GOES observations and MM5 output at a specified time (equation (5)). The slope is plotted in Figure 7 for each hour of the 10 day time sequence, along with slope values corresponding to the shifted MM5 grid having maximum correlation. A slope of one represents the best value of this statistic and is indicative of either no bias or a bias that is constant with UTRH. Any slope other than one implies that a bias dependent on UTRH

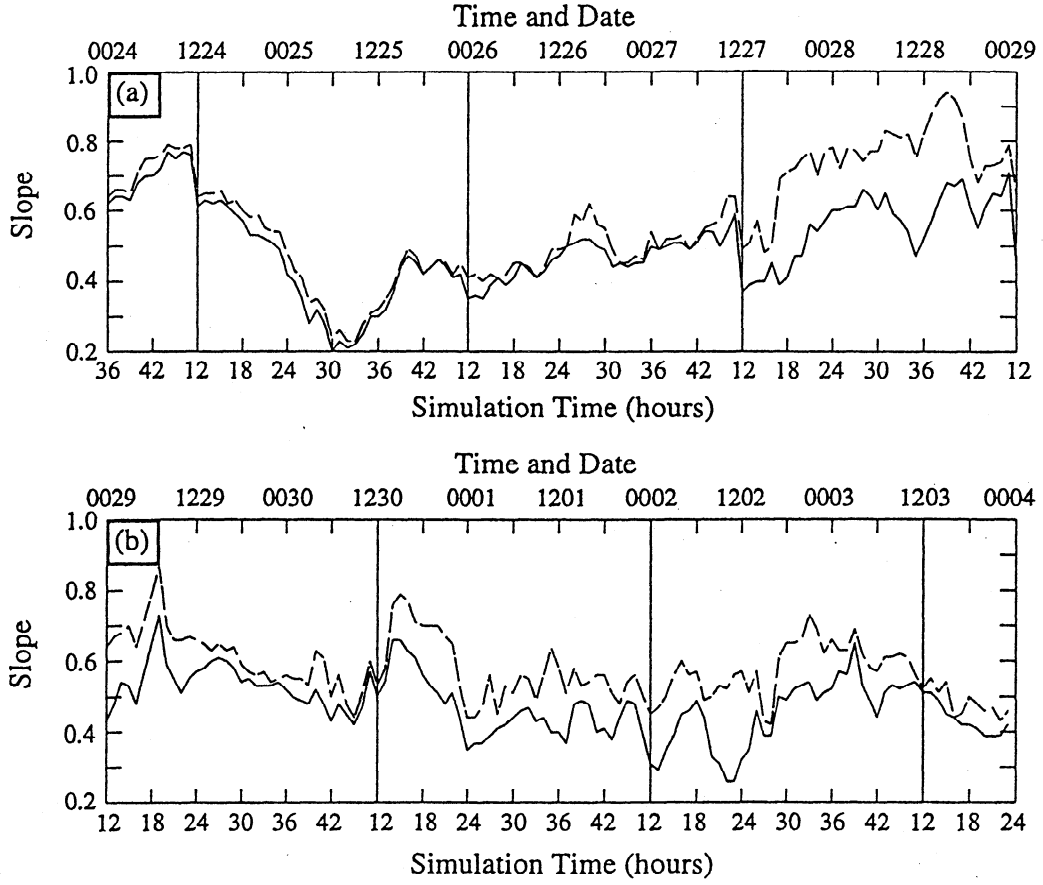

Figure 7. Same as Figure 5 but for the slope of the linear regression line between the MM5-UTRH simulations and the satellite data. (a) 0000 UTC November 24 to 0000 UTC November 29, 1991; (b) 0000 UTC November 29 to 2300 UTC December 3, 1991.

exists between the model and satellite-derived values and that this bias changes magnitude or sign in different areas over the computational domain. The fact that the UTRH slope values in Figure 7 are less than one, coupled with the model dry bias identified above, suggests that MM5 exhibits a stronger dry bias at higher relative humidities. A typical scatterplot of GOES versus MM5 $T_{6.7}$ and UTRH values valid at 1200 UTC November 26, 1991 is shown in Figure 8. A best fit linear regression line is plotted as well as the line that would result from a perfect agreement. Dry-biased MM5 values are concentrated on the right side of the UTRH scatterplot corresponding to higher than simulated GOES upper tropospheric relative humidities. In terms of $T_{6.7}$, dry biased data points (warmer $T_{6.7}$) are on the left side of the one-one line corresponding to lower-than-simulated GOES clear-sky 6.7μm brightness temperatures. A significant dry bias is observed over most of the domain while a moist bias is evident in those areas where the lowest GOES UTRH values exist. The slope is lowest from 1800 UTC November 24 to 1200 UTC November 25 (Figure 7) because MM5 is strongly dry biased in the broad area where it failed to capture a large maximum in the water vapor field. With respect to shifts in the MM5 grid, Figure 7 indicates that the slope usually improves (approaches one) for the appropriate shifts in the MM5 grid indicated in Figure 4. The improvement in the slope for the appropriate shift in the MM5 grid is most evident from 1200 UTC November 27 to 1800 UTC November 28 and occurs at a time when the dry bias is removed, and the bias standard deviation significantly improves for that shift in the MM5 grid which maximizes the correlation coefficient (compare Figures 5a, 6a, and 7a).

3.5 Discussion

It is the comparison of the statistics that allows for a thorough evaluation of model performance. For example, COR may be 1.0, for which case BSD and slope are 0.0 and 1.0, respectively. This would indicate that MM5 simulates perfectly the spatial features in the UTRH field. However, a constant non zero bias may exist. The slope of the linear regression line is necessary to determine whether or not any bias is constant over the domain. There could also be a case where no bias is present but there may be a large scatter in the data. The low UTRH COR from 2100 UTC November 24 to 1500 UTC November 25 (Figure 4c) occurs at a time when the dry bias becomes smaller (Figure 5), BSD is high (Figure 6), and the slope is low (Figure 7). Taken together, the statistics show that MM5 performance is poor, with the removal of the dry bias likely occurring because of a moist bias developing in low GOES UTRH areas. The maximum in correlation at 0600 UTC November 28 (Figure 4c) indicates that MM5 simulated accurately the spatial pattern in the UTRH field. However, a dry bias of 10% exists with a 10% BSD. The slope is approximately 0.5, indicating that the dry bias is skewed toward high GOES UTRH areas. From 1200 UTC November 30 to 0000 UTC December 2, bias is small (see Figure 5), COR ranges between 0.5 and 0.6, and the slope is near 0.5. This combination of statistics indicates that the MM5 performance

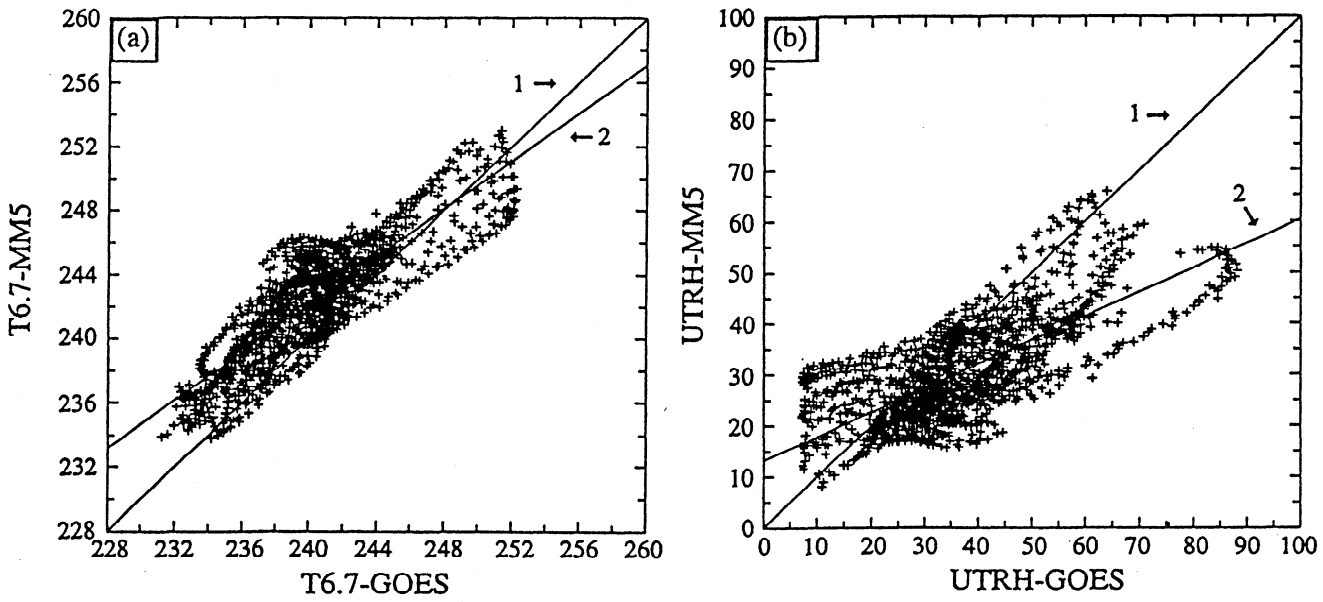

Figure 8. MM5 versus GOES scatter for 1200 UTC November 26, 1991. The line corresponding to the perfect model solution is shown (line) along with the linear regression line (line). (a) Clear-sky 6.7 m brightness temperatures; (b) upper tropospheric relative humidities.

was marginal with a large degree of scatter in the comparison between observation and simulation. During this period, a high degree of structure was evident in the UTRH fields, and these water vapor features advected rapidly through the analysis domain.

Overall, MM5 shows a reasonable skill at predicting the clear sky water vapor field in the upper troposphere. As an objective measure of this skill, we also examined the validation statistics assuming persistence of the UTRH fields. Figure 9 shows this comparison assuming persistence of the UTRH field from the beginning of the 12th hour of each model run during the first half of the simulation period. A perfect simulation is implied at the beginning of each comparison sequence since the UTRH field at that time is being compared to itself. The water vapor field changes rapidly, however, because of dynamical forcing and physical processes in the upper troposphere and the validation statistics degrade rapidly. Only on November 28 does the persistence assumption lead to a fortuitous forecast that approximates the skill of the model. During this period, a high degree of small-scale structure was present in the water vapor field over the analysis domain, and the persistence assumption reasonably approximated this structure.

Table 1 summarizes the statistics averaged over the 10 day period beginning 0000 UTC November 24 and ending on 2300 UTC December 3, 1991. As indicated by the average correlation coefficient of 0.80 for $T_{6.7}$ or 0.65 for UTRH, MM5 accurately predicts the locations of relative maxima and minima in the upper tropospheric water vapor field. Shifting the MM5 grid relative to the GOES grid produces only slight improvements in the statistics (Table 1). This is further evidence of the ability of MM5 to simulate and correctly predict the locations of most upper-tropospheric water vapor features. An average -3.3% UTRH dry bias in the upper troposphere was found with an 11% standard deviation. This bias is at least partially caused by MM5 being initialized with only 10% relative humidity in the model layers above 300 mbar. The dry bias tends to be more pronounced at the beginning of MM5 model runs when the dynamics are weak and in areas where the GOES UTRH is high. The notable changes in the statistics for shifts in the MM5 grid from 1200 UTC November 29 to 1200 UTC December 3 occur because of the lack of GOES data available (less than 10% at times) for the statistical analysis. Consequently, large changes in the statistics for the shifted relative to the unshifted MM5 grid are not representative of the ability of MM5 to simulate upper tropospheric water vapor features.

4. Conclusions

Since use of mesoscale models to simulate the water cycle in the upper troposphere is an important step toward understanding the physical processes that control the upper tropospheric water budget, we examined the skill of MM5 to simulate the clear sky UTRH during 10 days of the Project FIRE II field deployment. Validation was performed using GOES 7 6.7 μm radiance observations. Using the thermodynamic profiles predicted by the model at each grid point, a forward calculation of the radiance that would be observed by the satellite radiometer was performed, and comparison was made between simulation and observation. The radiances (simulated and observed) were converted to UTRH using the technique described by SB93. In general, MM5 performed well, faithfully simulating the pattern of UTRH during most of the period examined. Several situations were identified, however, when the overall MM5 performance was poor. These situations were associated with relatively weak dynamical forcing or with a large degree of small scale structure in the UTRH fields.

We found that MM5 has a well-defined dry bias in the upper troposphere. While this may be due, at least in part, to the microphysical parameterizations in the model, the practice of arbitrarily initializing the model above 300 mbar with 10% relative humidity likely contributed substantially to this effect. The dry bias was most evident during periods when the dynamical forcing was relatively weak. During periods of stronger dynamics, the model was able to recover a realistic water vapor field by about the twelfth hour of the integration.

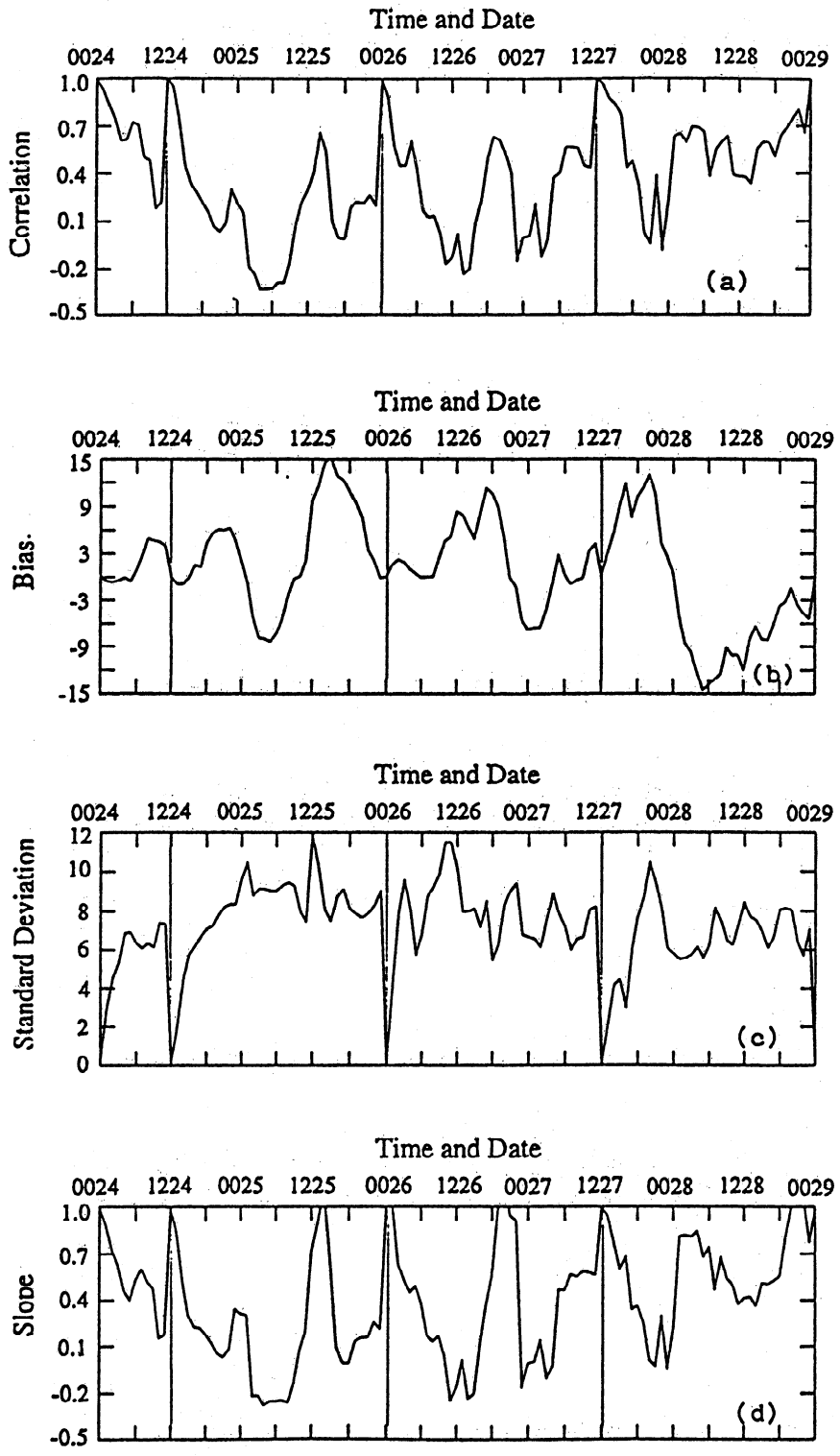

Figure 9. Validation statistics for UTRH assuming persistence for the first half of the simulation period. The GOES-observed UTRH grid at each hour is compared to the UTRH observations at the beginning of the comparison period. For example, all UTRH observations between 1200 UTC November 24 and 2300 UTC November 26 are compared to the observations at 1200 UTC November 24 Note that the ordinate range is expanded compared to the model validation figures. a) The linear correlation coefficient; (b) the bias; (c) the bias standard deviation; and (d) the slope of the linear regression line.

Table 1. Average Statistical Values During the 10 Day MM5 Evaluation Period

Statistic	$T_{6.7}$	$T_{6.7}S$	UTRH	UTRHS
COR	0.80	0.86	0.65	0.73
Bias	1.6K	1.7K	-3.3%	-2.7%
Bsd	2.8K	2.3K	11.4%	9.8%
Slope	0.82	0.90	0.49	0.58

$T_{6.7}S$ and UTRHS refer to the shifted MM5 $T_{6.7}$ and UTRH grids that produce the best correlation with the GOES observations.

Furthermore, it is evident that this problem would occur for any arbitrarily assumed relative humidity during periods when the vertical coupling between the upper troposphere and lower troposphere is weak. Given this, it is clear that the only solution to this problem is to initialize and nudge the model with accurate UTRH measurements. This is especially critical when models of this type are being used to examine the coupling between physical processes and the model dynamics in the upper troposphere. The immediate solution is to begin using 6.7 μm satellite data in clear sky for initialization and assimilation of mesoscale models. As we and others have shown, these observations provide an accurate measure of UTRH and can be used effectively as a model diagnostic.

A second problem identified in our evaluation of MM5-UTRH simulations is the tendency for the model to underestimate extrema in the UTRH field. We suggest that this is a result of the relatively coarse vertical resolution typical of numerical weather prediction models in the upper troposphere (1.5 km). Because of this coarse vertical resolution, strong mesoscale dynamic features responsible for the existence of exceptionally moist or dry regions in the upper troposphere tend to be subdued. Increased vertical resolution in the upper troposphere, coupled with an overall improvement in UTRH due to the use of 6.7 μm data for initialization and data assimilation, would certainly improve simulations of the formation and evolution of cirrus clouds.

Acknowledgments. We wish to thank David R. Stauffer and Mark Leidner for their advice and suggestions in the area of mesoscale numerical weather prediction. Zitian Guo carried out the mesoscale model simulations that were used in this project. Glen Hunter and Mark Leidner provided invaluable help in retrieving and processing the mesoscale model output. We appreciate the generosity of Hal Woolf in providing us with the CIMSS transmittance model code. Research funding was provided by NASA grants NAG-1-999 and NAG-1-1095. Computer resources were supplied by the Earth System Science Center of Pennsylvania State University.

References

Ackerman, S.A., R.A. Frey, and W.L. Smith, Radiation budget studies using collocated observations from Advanced Very High Resolution Radiometer, High-Resolution Infrared Sounder/2, and Earth Radiation Budget Experiment instruments. *J. Geophys. Res., 97*, 11513-11525, 1992.

Akima, H., A method of bivariate interpolation and smooth surface fitting for values given at irregularly distributed points, *ACM-TOMS, 4*, 148-159, 1978.

Akima, H., On estimating partial derivatives for bivariate interpolation of scattered data, *Rocky Mtn. J. Math, 14*, 41-52, 1984.

Anthes, R.A., Regional models of the atmosphere in middle latitudes, *Mon. Weather. Rev., 111*, 1306-1334, 1983.

Dudhia, J., A nonhydrostatic version of the Penn State-NCAR Mesoscale Model: Validation tests and simulation of an Atlantic cyclone and cold front, *Mon. Wea. Rev., 121*, 1493-1513, 1993.

First International Satellite Cloud Climatology Project Regional Experiment Project Office, FIRE Phase III Research Plan, report, 141 pp., NASA Langley Res. Cent, Hampton, Va., 1994.

Grell, G.A., J. Dudhia, and D.R. Stauffer, A description of the fifth-generation Penn State/NCAR Mesoscale Model (MM5)., *NCAR Tech. Note NCAR/TN-398+STR*, 138 pp., Nat. Cent. for Atmos. Res., Boulder, C., 1994.

Guo, Z., Evaluation of cloud prediction and determination of critical relative humidity for a mesoscale numerical weather prediction model, M.S. thesis, 132 pp., Pa. State Univ., University Park, 1994.

Larsen, J.C., E.W. Chieu, W.P. Chu, M.P. McCormick, L.R. McMaster, S. Oltmans, and D. Rind, A comparison of the stratospheric aerosol and gas experiment II tropospheric water vapor to radiosonde measurements, *J. Geophys. Res., 98*, 4897-4917, 1993.

Mace, G.G., Development of large-scale diagnostic analysis techniques applicable to regional arrays of wind profilers and radiosondes, Ph.D. thesis, 262 pp., Pa. State Univ., University Park, 1994.

Menzel, W.P., W.L. Smith, and L.D. Herman, Visible infrared spin-scan radiometer atmospheric sounder radiometric calibration: An in-flight evaluation from intercomparison with HIRS and radiosonde measurements, *Appl. Opt., 15*, 358-363, 1981.

Schmetz, J., and O.L. Turpeinen, Estimation of the upper-tropospheric relative humidity field from Meteosat water vapor image data, *J. Clim. Appl. Meteorol., 27*, 889-899, 1988.

Soden, B.J., and F. Bretherton, Upper tropospheric relative humidity from the GOES 6.7 m channel: Method and climatology for July 1987, *J. Geophys. Res., 98*, 16669-16687, 1993.

Soden, B.J., and F. Bretherton, Evaluation of water vapor distribution in general circulation models using satellite observations, *J. Geophys. Res., 99*, 1187-1210, 1994.

Soden, B.J., S.A. Ackerman, D.O'C. Starr, S.H. Melfi, and R.A. Ferrare, Comparison of upper tropospheric water vapor from GOES, Raman lidar, and cross-chain loran atmospheric

sounding system measurements, *J. Geophys. Res., 99*, 21005-21016, 1994.

Starr, D.O'C., Numerical experiments on the formation and maintenance of cirriform clouds., Ph.D. thesis, 351 pp., Colo. State Univ., Fort Collins, 1985.

Stauffer, D.R., and N.L. Seaman, Use of four-dimensional data assimilation in a limited-area mesoscale model, 1, Experiments with synoptic-scale data, *Mon. Weather Rev., 118*, 1250-1277, 1990.

Tarbell, T.C., T.T. Warner, and R.A. Anthes, An example of the initialization of the divergent wind component in a mesoscale numerical weather prediction model, *Mon. Weather Rev., 109*, 77-95, 1981.

Van De Berg, L., A. Pyomjamsri, and J. Schmetz, Monthly mean upper tropospheric humidities in cloud-free areas from Meteosat observations, *Int. J. Climatol., 11*, 819-826, 1991.

Westphal, D. L., et al., Initialization and validation of a simulation of cirrus using FIRE II data, *J. Atmos. Sci., 53*, 3397-3429, 1996.

Wu, X., J.J. Bates, and S.J.S. Khalsa, A climatology of the water vapor band brightness temperatures from NOAA operational satellites, *J. Clim., 6*, 1282-1299, 1993.

T. P. Ackerman and N. L. Seaman, Department of Meteorology and Earth System Science Center, Pennsylvania State University, University Park, PA 16802. (email: ackerman@essc.psu.edu; seaman@psumeteo.psu.edu)

G. G. Mace, Department of Meteorology, University of Utah, 819 Wm. C. Browning Bldg., Salt Lake City, UT 84112. (email: mace@atmos.met.utah.edu)

B.J. Soden, Geophysical Fluid Dynamics Laboratory, NOAA, Princeton, NJ 08540.

D.A. Spangenberg, NASA Langley Research Center, One Enterprise Parkway, Hampton, VA 23681. (email: doug@vikranth.larc.nasa.gov).

(Received, February 13, 1996; revised, November 21, 1996; accepted, May 22, 1997.)